crystals

MDPI

Article

Mechanical and Electronic Properties of DNTF Crystals under Different Pressure

Hai Nan [1,2], Xianzhen Jia [2], Xuanjun Wang [1,*], Heping Liu [3], Fan Jiang [2] and Peng Zhang [2]

[1] High-Tech Institute of Xi'an, Xi'an 710025, China; walese_2000@sina.com
[2] Xi'an Modern Chemistry Research Institute, Xi'an 710065, China; jiaxz@163.com (X.J.); jiangfan9101@163.com (F.J.); zhangpengz@stu.xjtu.edu.cn (P.Z.)
[3] School of Material Science and Engineering, North University of China, Taiyuan 030051, China; peace666@126.com
* Correspondence: wangxj503@sina.com

Abstract: In the present study, the effects of pressure on the structure, elastic properties and electronic structure of DNTF compounds are studied using the first principles method. It is found that pressure has a great influence on lattice constants. When the pressure reaches 80 GPa, the structure of DNTF changes suddenly. The variation trend of C_{11}, C_{22} and C_{33} values is consistent with that of pressure. In addition, pressure can improve the compressibility and shear resistance of the DNTF compound. The pressure can reduce the bandgap and further increases the charge density, causing DNTF to decompose and explode.

Keywords: DNTF; different pressure; lattice constant; mechanical properties; electronic properties

Citation: Nan, H.; Jia, X.; Wang, X.; Liu, H.; Jiang, F.; Zhang, P. Mechanical and Electronic Properties of DNTF Crystals under Different Pressure. *Crystals* **2021**, *11*, 1180. https://doi.org/10.3390/cryst11101180

Academic Editors: Alexander Y. Nazarenko and Shujun Zhang

Received: 7 September 2021
Accepted: 25 September 2021
Published: 28 September 2021

1. Introduction

Furoxan derivatives are a class of important energetic materials, which have attracted extensive attention due to their high density, good oxygen balance, good detonation performance and high thermal stability [1–6]. 3, 4-bis (3-nitrofurazan-4-yl) furoxan (DNTF) is a compound of furoxan derivatives, with high energy, low melting point and excellent comprehensive properties. As a promising high energy density material (HEDM), DNTF has become the focus of energetic materials researchers in recent years [7–11]. It is of great significance to study the properties of DNTF since the properties of this material directly affect its use, transportation and storage.

In order to further improve the comprehensive performance of DNTF, domestic and foreign researchers have carried out continuous exploration. Sinditskii V P et al. [12] performed thermal decomposition under isothermal conditions. The final study found that the thermal stability of DNTF was close to 1, 3, 5, 7-tetranitro-1, 3, 5, 7-tetrazocane (HMX), and the combustion rate was close to that of 2, 4, 6, 8, 10, 12-hexanitro-2, 4, 6, 8, 10, 12-hexaazaisowurtzitane (CL-20). Song et al. [13] studied the effect of methanol and acetic acid/aqueous solution on the crystal morphology of DNTF. The results showed that (001), (111), and ($11\bar{1}$) crystal faces were mainly exposed, while (011), (101), and (110) faces disappeared or occupied small areas. These results can provide theoretical support for the crystallization process of DNTF. Kazakov et al. [14] have meticulously researched the thermochemical and energy characteristics of DNTF and DNFF as composite solid rocket propellants. When used for aluminum-free and active binder-containing components, DNTF can provide a specific impulse of 254.5 s at 40 and 1 atm pressure at the combustion chamber and nozzle exit, respectively. Gu et al. [15] studied the thermal decomposition kinetics of DNTF using differential scanning calorimetry (DSC) test. The results showed that the decomposition mainly consisted of exothermic peaks P1, P2 and P3, which could be described by the N-order reaction model.

Furthermore, Wu et al. [16] studied the effects of high pressure on the structure, electron and absorption properties of 2, 6-diamino-3, 5-dinitropyrazine-1-oxide (LLM-105)

by using first principles. The density of states analysis demonstrates that the interaction between valence electrons is enhanced under pressure. The p orbital plays an important role in the chemical reaction of LLM-105. Wang et al. [17] studied the structure, electron and thermodynamic properties of 4, 4′, 6, 6′-tetra (azido) azo-1, 3, 5-triazine (TAAT) under pressure by using the first principles method. The study shows that the bandgap is almost zero when the pressure is 70 GPa. This indicates that TAAT has metallic properties at this time. The density of states shows that electron delocalization generally increases in TAAT under the influence of pressure. This result indicates that the impact sensitivity can be improved by applying pressure.

However, the effect of pressure on DNTF performance has not been reported. In addition, it is of great significance to study the mechanical and electronic properties of DNTF under different pressures. Therefore, in this study, the effects of different pressures on the crystal structure, mechanical properties and electronic properties of DNTF were studied using first principles.

2. Materials and Methods

In this paper, the study of DNTF performance was conducted by using the Cambridge serial total energy package (CASTEP) software package based on density functional theory [18,19]. In order to obtain the most stable structure, the Broyden–Flecher–Goldfarb–Shanno (BFGS) [20] method was used for the geometric optimization of the crystal structure. Perdew–Burke–Ernzerhof (PBE) [21] in the generalized gradient approximation (GGA) can be selected for the commutative association. The ultrasoft pseudopotentials (USP) were selected as pseudopotentials. When optimizing the crystal structure, the convergence precision was set as: SCF 5.0 $\times$ 10^{-7} eV/atom, the total energy 1.0 $\times$ 10^{-5} eV/atom, the force on each atom 0.03 eV/Å, the maximum displacement 0.001Å and the maximum stress deviation 0.05 GPa. After the convergence test and considering the computational efficiency, the energy cut-off was 480 eV and the k-point was 5 $\times$ 3 $\times$ 2.

In order to study the change of DNTF structure with pressure, optimization calculation was carried out in the range of 0–80 GPa with step size of 10 GPa. The molecular formula of DNTF is $C_6N_8O_8$ and its chemical structural formula is shown in Figure 1a. The crystal structure belongs to orthogonal crystal and the space group is $P2_12_12_1$ (No.19), as shown in Figure 1b).

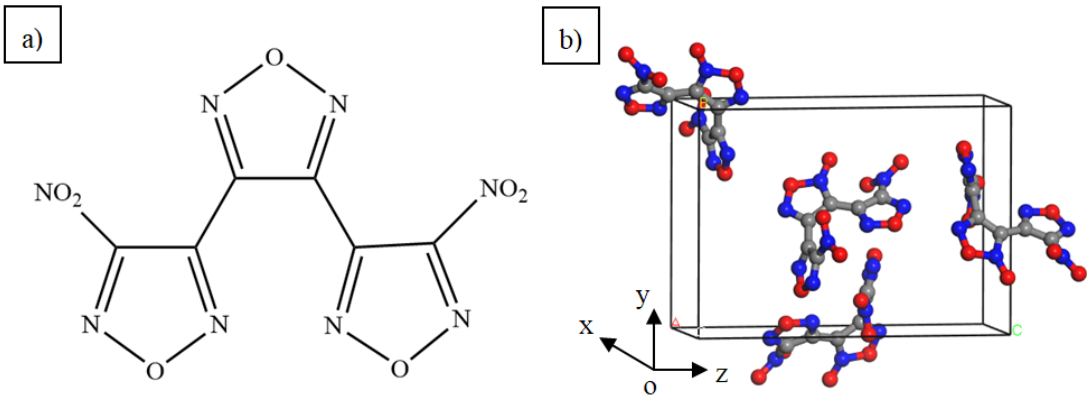

Figure 1. The structure of DNTF. (**a**) The chemical structure; (**b**) The crystal structure.

3. Results

3.1. Lattice Constants and Stability

The calculated lattice constants of DNTF in 0 K and 0 GPa ground state are listed in Table 1. It can be seen that the lattice constants calculated at the ground state are in good agreement with the experimental values [22], indicating that the calculation method and simulation results adopted are accurate and reasonable. As can be seen from Table 1, in the range of 0–80 GPa, the lattice constants (a and c) of DNTF decrease with increasing

pressure. However, when the pressure is 80 GPa, the lattice constant (b) increases suddenly, suggesting that the structure of the compound changes at this time.

Table 1. The calculated lattice parameters of DNTF under different pressure.

Pressure	a(Å)	b(Å)	c(Å)
0 GPa	6.821	10.983	15.410
Exp. [22]	6.662	10.740	15.093
10 GPa	5.847	10.381	14.132
20 GPa	5.519	10.154	13.618
30 GPa	5.311	9.994	13.315
40 GPa	5.164	9.872	13.074
50 GPa	5.039	9.775	12.900
60 GPa	4.922	9.714	12.748
70 GPa	4.820	9.703	12.548
80 GPa	4.760	9.874	12.090

With the aim to intuitively show the influence of pressure on the structure of the DNTF compound, the relationship between lattice constant changes and pressure is shown in Figure 2. As displayed in the figure, the change rate of the lattice constant of DNTF gradually decreases with the increase of pressure. When the pressure increases from 0 to 80 GPa, the change rate of lattice constant a (a/a_0) of DNTF changes most obviously, decreasing to 0.658. It means that the a-direction is more sensitive to pressure in the crystal structure of DNTF. Moreover, with the increase of pressure, the decreasing trend of a/a_0, b/b_0 and c/c_0 tends to be slower. This is because the distance between atoms in DNTF crystal decreases with the increase of pressure, which leads to the increasing of interatomic repulsion force. In particular, when the pressure reaches 80 GPa, the value of b/b_0 increases suddenly from 0.843 at 70 GPa to 0.858. On the contrary, the decreasing degree of c/c_0 suddenly increased, demonstrating that the structure of DNTF changed at this point.

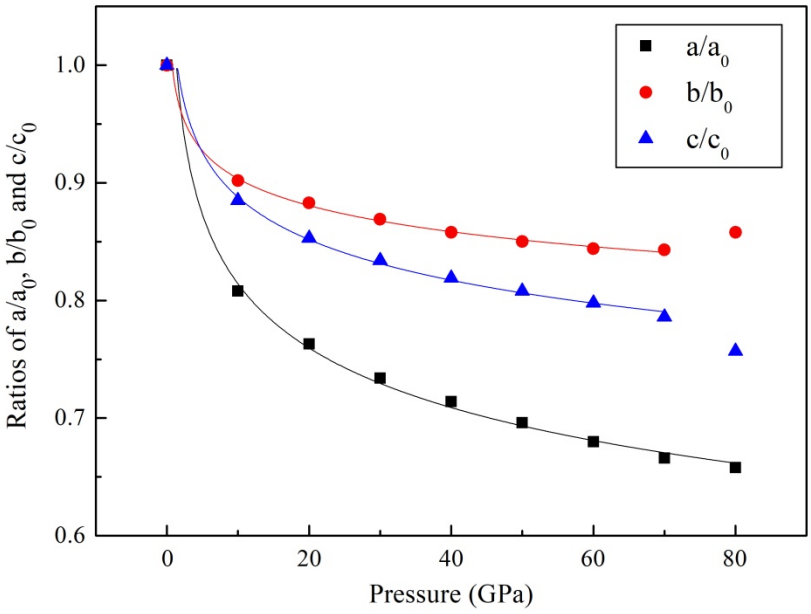

Figure 2. The lattice constant changes of DNTF under different pressure.

The power equation is obtained by curve fitting of the existing data, according to which the influence of pressure on the lattice constant of DNTF can be fully understood. It is noteworthy that the crystal structure changes and the lattice constants (b and c) change abnormally when the pressure is 80 GPa. Therefore, when fitting b/b_0 and c/c_0 curves, the

range of pressure is selected as 0–70 GPa. The fitting curves are shown in Figure 2 and the fitting formulas are as follows:

$$a/a_0 = 1.02231 \times P^{-0.09919}, \quad (1)$$

$$b/b_0 = 0.98313 \times P^{-0.03672}, \quad (2)$$

$$c/c_0 = 1.01770 \times P^{-0.05940}, \quad (3)$$

3.2. Mechanical Properties

The elastic constants play an important role in the mechanical and thermodynamic properties of materials. It is well known that orthogonal crystals have nine independent elastic constants, which are C_{11}, C_{22}, C_{33}, C_{44}, C_{55}, C_{66}, C_{12}, C_{13} and C_{23}. The mechanical stability of compounds with orthorhombic structure can be judged according to formula (4) [23]

$$\begin{gathered} C_{11} > 0, C_{22} > 0, C_{33} > 0, C_{44} > 0, C_{55} > 0, C_{66} > 0, \\ [C_{11} + C_{22} + C_{33} + 2(C_{12} + C_{13} + C_{23})] > 0, \\ (C_{11} + C_{22} - 2C_{12}) > 0, (C_{11} + C_{33} - 2C_{13}) > 0, \\ (C_{22} + C_{33} - 2C_{23}) > 0. \end{gathered} \quad (4)$$

where, C_{ij} is the elastic constant.

In this work, the elastic constants of DNTF compounds under different pressures are calculated. According to formula (4), it can be judged that DNTF is mechanically stable at 0 GPa, as shown in Table 2. In order to show the influence of pressure on the elastic constant more intuitively, the variation trend of the elastic constant with pressure was plotted, as shown in Figure 3. Based on the previous results of lattice constant, the structure of DNTF changes when the pressure is 80 GPa. Therefore, the influence of pressure on performance in the range of 0–70 GPa is discussed in the following research. As can be seen from Figure 3, C_{11}, C_{22} and C_{33} show the same trend of change and their values increase with the enhancement of pressure. With the increase of pressure, the value of C_{66} is consistent with its change trend, but the trend of C_{44} and C_{55} is different. When the pressure is 50 GPa, the values of C_{44} and C_{55} reach 35.99 GPa and 17.78GPa, respectively. As the pressure continues to increase, these value decreases. The increase in elastic constants C_{12}, C_{13} and C_{23} is the same as the change in the trend of pressure. When the pressure is greater than 50 GPa, the value of C_{13} increases more slowly than that of C_{12} and C_{23}.

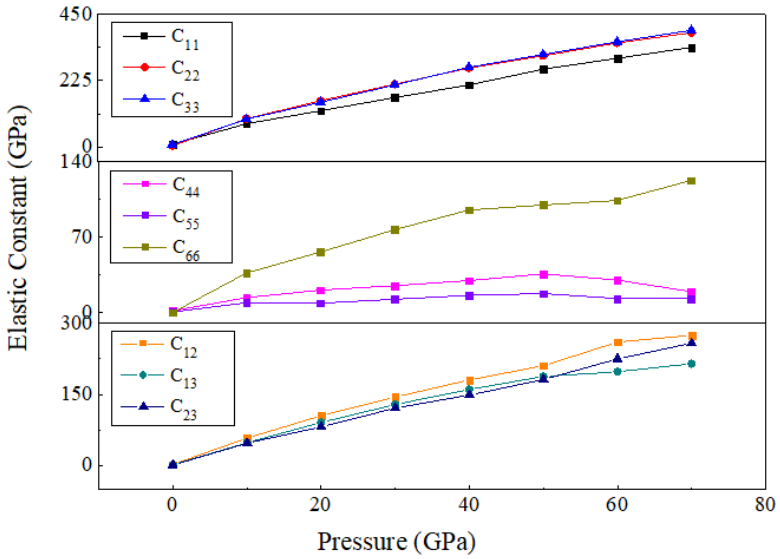

Figure 3. The elastic constants of DNTF under different pressure.

Table 2. The calculated elastic constants of DNTF at 0 GPa.

Phase	Species	C_{11}	C_{12}	C_{13}	C_{22}	C_{23}	C_{33}	C_{44}	C_{55}	C_{66}
DNTF	Present	8.70	1.75	1.09	3.39	0.70	7.40	1.72	0.63	0.07

The bulk modulus (B), shear modulus (G), Young's modulus (E) and Poisson's ratio (υ) of DNTF compound can be calculated by the following equations [24,25]:

$$B_H = \frac{1}{2}(B_V + B_R) \tag{5}$$

$$G_H = \frac{1}{2}(G_V + G_R) \tag{6}$$

$$E = \frac{9B_H G_H}{(3B_H + G_H)} \tag{7}$$

$$\sigma = \frac{(3B_H - 2G_H)}{[2(3B_H + G_H)]} \tag{8}$$

For orthorhombic materials [26,27]:

$$B_V = \frac{1}{9}(C_{11} + C_{22} + C_{33}) + \frac{2}{9}(C_{12} + C_{13} + C_{23}) \tag{9}$$

$$B_R = 1/[(S_{11} + S_{22} + S_{33}) + 2(S_{12} + S_{13} + S_{23})] \tag{10}$$

$$G_V = \frac{1}{15}(C_{11} + C_{22} + C_{33}) - \frac{1}{15}(C_{12} + C_{13} + C_{23}) + \frac{3}{15}(C_{44} + C_{55} + C_{66}) \tag{11}$$

$$G_R = 1/\left[\frac{4}{15}(S_{11} + S_{22} + S_{33}) - \frac{4}{15}(S_{12} + S_{13} + S_{23}) + \frac{3}{15}(S_{44} + S_{55} + S_{66})\right] \tag{12}$$

where, B_V and B_R are bulk moduli calculated by Voigt and Reuss methods, which limit the maximum and minimum values of bulk moduli respectively. B_H is the bulk modulus calculated by the Hill method and is the average value of B_V and B_R. The shear moduli G_V, G_R and G_H are defined in the same way. S_{ij} is the elastic compliances constant.

Figure 4 exhibits the pressure dependence of the bulk modulus, shear modulus, Young's modulus and Poisson's ratio of the compound DNTF. It is reasonable to conclude that the bulk modulus and shear modulus increase with the rise of pressure. This result suggests that increasing pressure can improve the compressibility and shear resistance of a DNTF compound. When the pressure is less than 50 GPa, the Young's modulus of the DNTF compound increases. However, when the pressure is greater than 50 GPa, the Young's modulus decreases. This phenomenon indicates that the stiffness of the DNTF compound is the maximum when the pressure is 50 GPa but it is not beneficial to the increase of compound stiffness when the pressure continues to increase. As the pressure increased from 0 GPa to 70 GPa, the Poisson's ratio of DNTF compound increases from 0.32 to 0.43. The result shows that increasing pressure can further improve the elasticity and reduce the brittleness of a DNTF compound. When the pressure reaches 30 GPa, the change of Poisson's ratio becomes gentle and the influence of pressure becomes small.

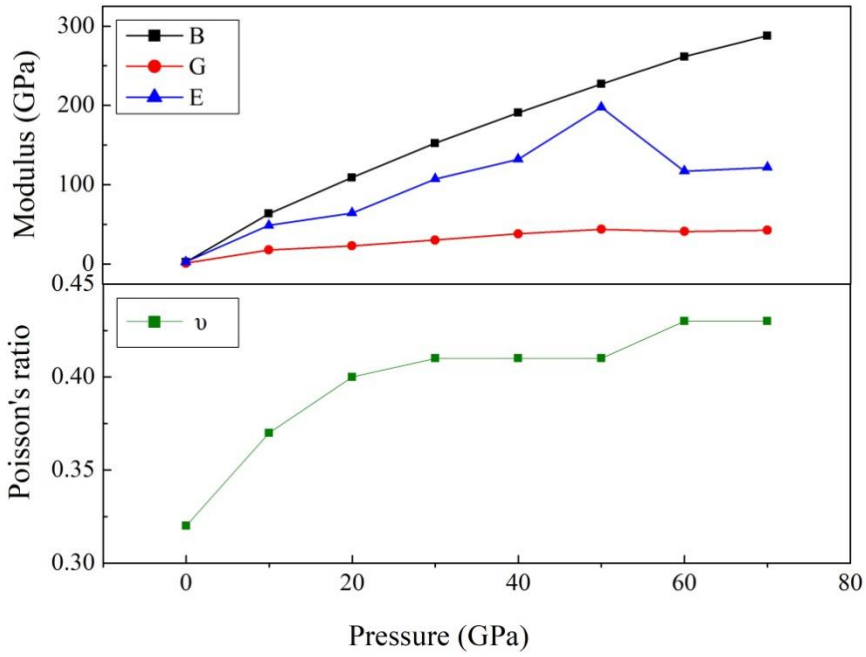

Figure 4. The modulus and Poisson's ratio of DNTF under different pressure.

3.3. Electronic Properties

In order to analyze the bonding properties between atoms in DNTF compounds and the effect of pressure on the chemical bonding in the structure, the total density of states (TDOS) and the partial density of states (PDOS) were calculated. The total density of states and the partial density of states at 0 GPa are shown in Figure 5. It can be observed from Figure 5, in the energy range from −8 to 0 eV and the conduction band part, the TDOS mainly comes from the p orbitals of O, N and C atoms. In addition, the TDOS is mainly derived from the s orbitals of O, N and C atoms in the low energy region.

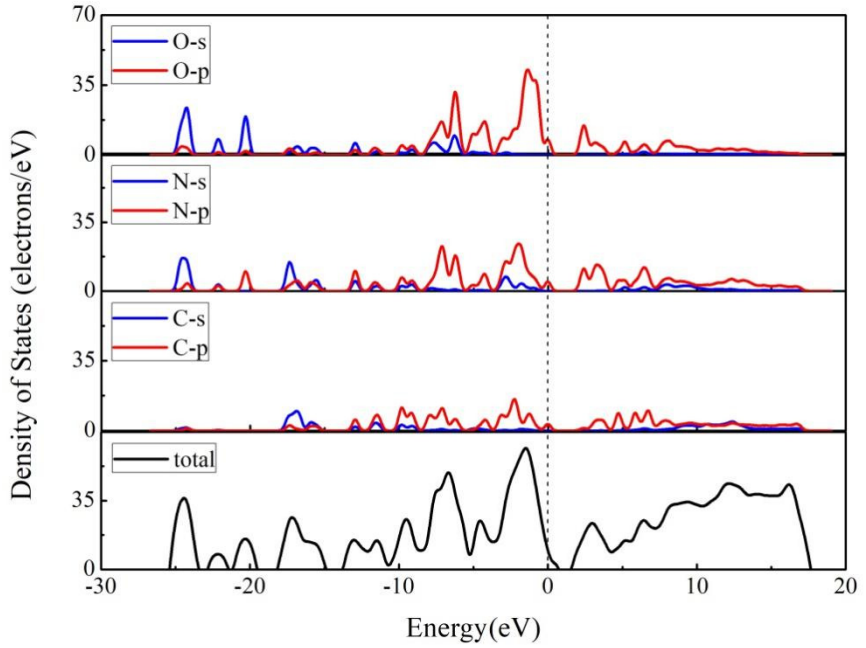

Figure 5. The density of states of DNTF at 0 GPa.

The TDOS under different pressures is shown in Figure 6, from which it can be seen that the curve and trend of the TDOS under different pressures are similar. The results demonstrate that the structure of DNTF is stable and there is no structural change within

the studied pressure range. As the pressure increases, the TDOS decreases, which is owing to the change of the interaction potential [28].

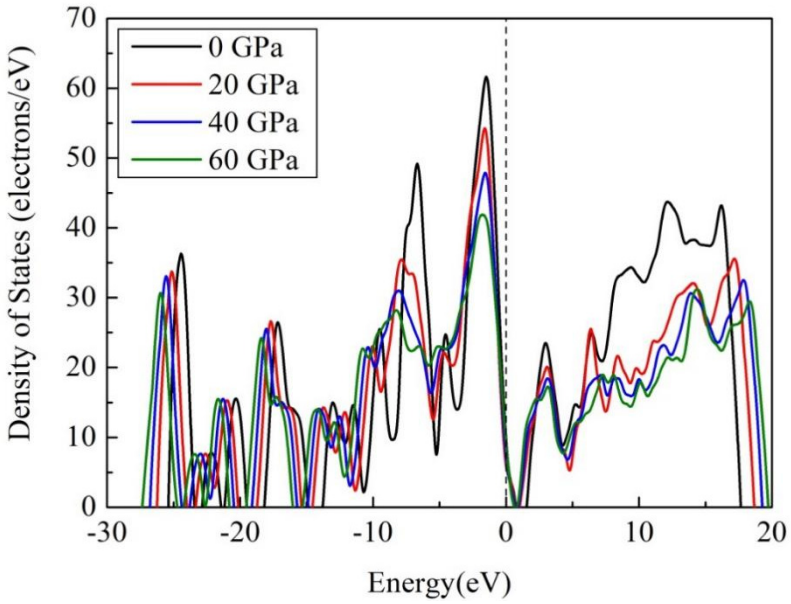

Figure 6. The density of states of DNTF under different pressure.

The bandgap is generally the energy difference between the bottom of the conduction band and the top of the valence band. As can be seen from Figure 6, the bandgap gradually decreases with the increase of pressure. In order to observe the change of the bandgap more intuitively, the change of the DNTF bandgap under different pressures is plotted in Figure 7. It can be clearly seen from Figure 7 that the bandgap gradually decreases as the pressure increases. When the pressure reaches 30 GPa, the decreasing trend of the bandgap becomes gentle. As the bandgap decreases, the electron more easily transitions from the valence band to the conduction band. This makes the material more likely to disintegrate and explode [29]. Therefore, it can be concluded that with the increase of pressure, DNTF is easier to decompose and its structure is more unstable.

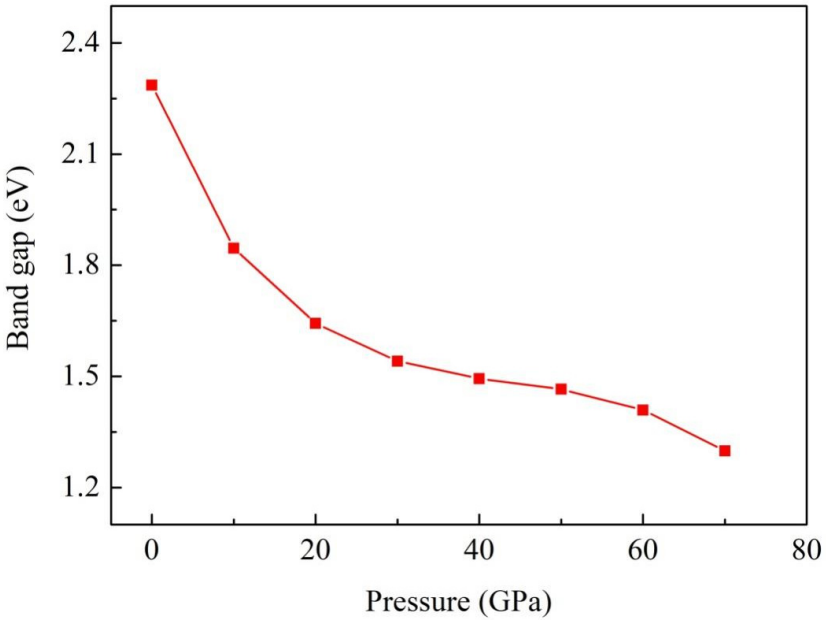

Figure 7. The bandgap of DNTF under different pressure.

In order to analyze the influence of pressure on the electron density in the DNTF compound in more detail, the electron density and electron density differences under different pressure are calculated. The electron density diagram can reflect the electron density around the atom in the DNTF compound. The influence of pressure on the charge density is shown in Figure 8, which is drawn in the range of 0–1 e/Å^3. With the increase of pressure, the electron density around the atom increases continuously. It can be seen that pressure promotes charge aggregation in DNTF compounds and increases electron density.

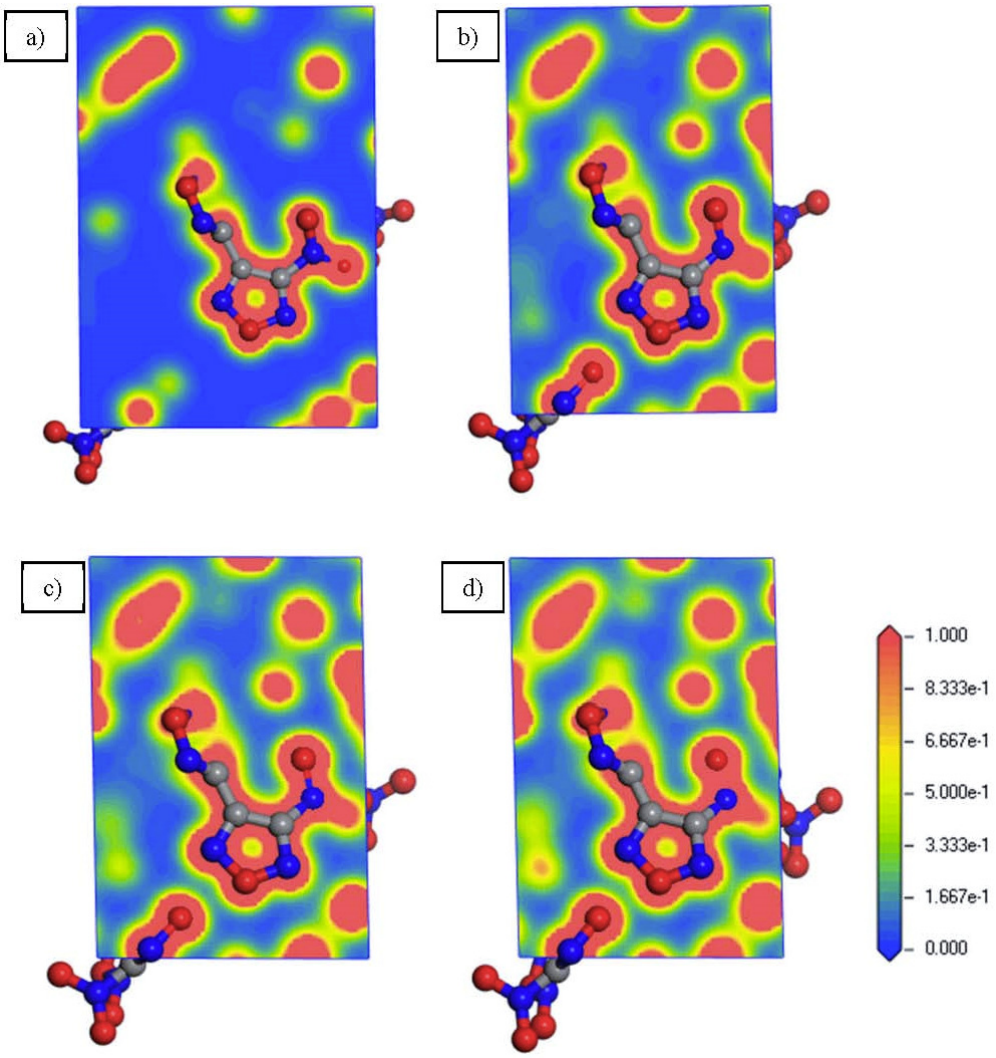

Figure 8. The electron density of DNTF under different pressure. (**a**) 0 GPa; (**b**) 20 GPa; (**c**) 40 GPa; (**d**) 60 GPa.

The electron density difference represents the gain and loss of electrons in a DNTF compound. The electron density difference of DNTF under different pressures is shown in Figure 9 and the plot range is −0.8–0.8 e/Å^3. In this figure, red means getting electrons and blue means losing electrons. In DNTF compounds, C atoms gain electrons and there is a shared electron between C-C bonds. With the increase of pressure, the degree of electron gain and loss does not change obviously. The degree of electron aggregation around N and O atoms increases. It leads to the further polarization of atomic binding bonds in DNTF compounds, which promotes the impact sensitivity of DNTF.

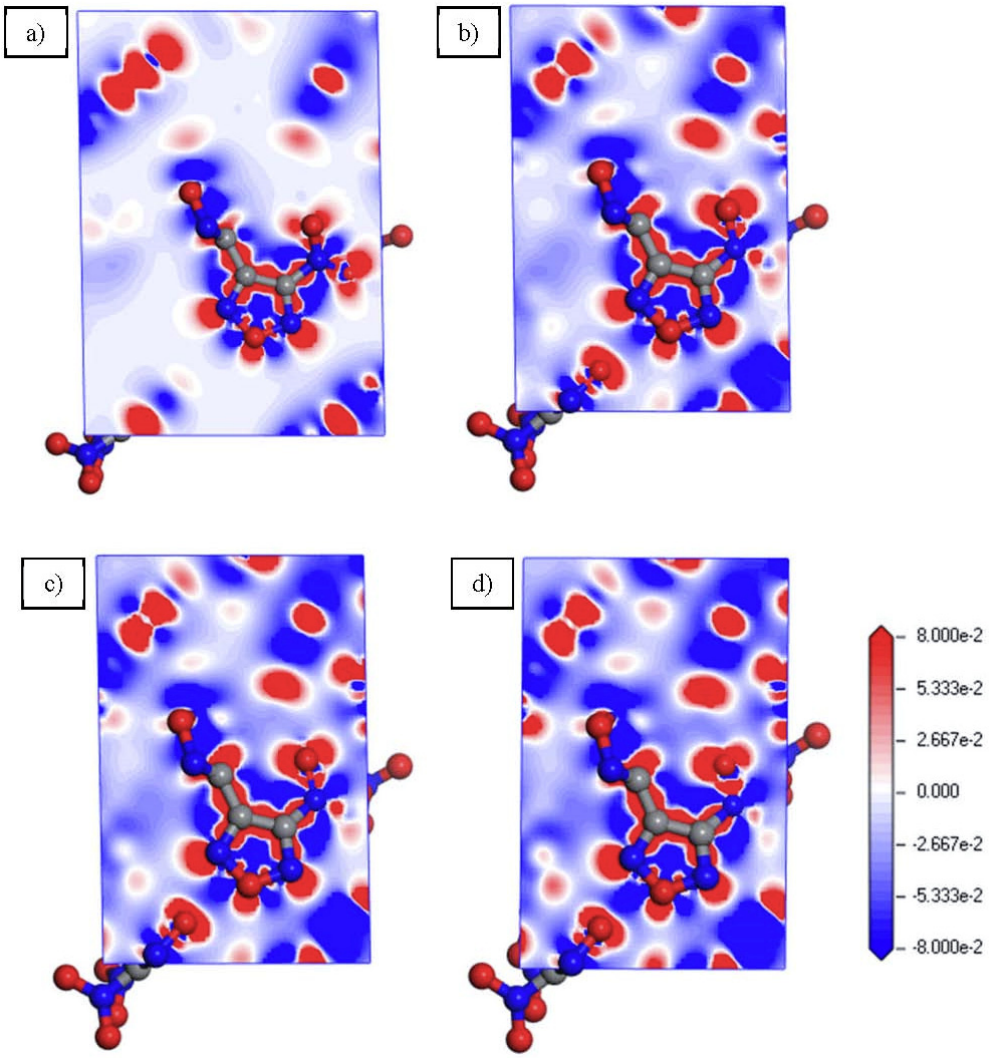

Figure 9. The electron density difference of DNTF under different pressure. (**a**) 0 GPa; (**b**) 20 GPa; (**c**) 40 GPa; (**d**) 60 GPa.

4. Conclusions

In this work, the effect of pressure on the structure, elastic properties and electronic structure of DNTF compound is studied. The lattice constant of DNTF decreases with increasing pressure. When the pressure reaches 80 GPa, the structure of DNTF changes. As the pressure increases, the values of C_{11}, C_{22} and C_{33} increase. The bulk modulus and shear modulus increase with the increase of pressure. The results show that pressure is helpful to improve the compressibility and shear resistance of DNTF compounds. With the enhancement of pressure, the bandgap decreases gradually, which increases the possibility of material decomposition and explosion. The electron aggregation around N and O atoms increases, which improves the impact sensitivity of DNTF.

Author Contributions: Conceptualization, H.N. and X.J.; methodology, H.N.; software, X.W.; validation, H.L., F.J.; formal analysis, H.N. and X.J.; investigation, H.N. and X.J.; resources, X.W.; data curation, H.N.; writing—original draft preparation, H.N.; writing—review and editing, X.W. and P.Z.; visualization, P.Z.; supervision, X.W. All authors have read and agreed to the published version of the manuscript.

Funding: This research received no external funding.

Conflicts of Interest: The authors declare no conflict of interest.

References

1. Zhang, J.; Zhou, J.; Bi, F.; Wang, B. Energetic materials based on poly furazan and furoxan structures. *Chin. Chem. Lett.* **2020**, *31*, 2375–2394. [CrossRef]
2. Ji, J.; Zhu, W. Thermal decomposition mechanisms of benzotrifuroxan: 2, 4, 6-trinitrotoluene cocrystal using quantum molecular dynamics simulations. *Chem. Phys. Lett.* **2021**, *778*, 138820. [CrossRef]
3. Wu, C.-L.; Zhang, S.-H.; Gou, R.-J.; Ren, F.-D.; Han, G.; Zhu, S.-F. Theoretical insight into the effect of solvent polarity on the formation and morphology of 2, 4, 6, 8, 10, 12-hexanitrohexaazaisowurtzitane (CL-20)/2, 4, 6-trinitro-toluene (TNT) cocrystal explosive. *Comput. Theor. Chem.* **2018**, *1127*, 22–30. [CrossRef]
4. Larin, A.A.; Shaferov, A.V.; Epishina, M.A.; Melnikov, I.N.; Muravyev, N.V.; Ananyev, I.V.; Fershtat, L.L.; Makhova, N.N. Pushing the energy-sensitivity balance with high-performance bifuroxans. *ACS Appl. Energy Mater.* **2020**, *3*, 7764–7771. [CrossRef]
5. Xiong, H.; Cheng, G.; Zhang, Z.; Yang, H. C 8 n 12 o 10: A promising energetic compound with excellent detonation performance and desirable sensitivity. *New J. Chem.* **2019**, *43*, 7784–7789. [CrossRef]
6. He, C.; Gao, H.; Imler, G.H.; Parrish, D.A.; Shreeve, J.M. Boosting energetic performance by trimerizing furoxan. *J. Mater. Chem. A* **2018**, *6*, 9391–9396. [CrossRef]
7. Zhao, F.; Chen, P.; Hu, R.; Yang, L.; Zhang, Z.; Zhou, Y.; Yang, X.; Gao, Y.; Gao, S.; Shi, Q. Thermochemical properties and non-isothermal decomposition reaction kinetics of 3, 4-dinitrofurazanfuroxan (DNTF). *J. Hazard. Mater.* **2004**, *113*, 67–71.
8. Xu, C.; An, C.; He, Y.; Zhang, Y.; Li, Q.; Wang, J. Direct ink writing of DNTF based composite with high performance. *Propellants Explos. Pyrot.* **2018**, *43*, 754–758. [CrossRef]
9. Liu, N.; Zeman, S.; Shu, Y.; Wu, Z.; Wang, B.; Yin, S. Comparative study of melting points of 3, 4-bis (3-nitrofurazan-4-yl) furoxan (DNTF)/1, 3, 3-trinitroazetidine (TNAZ) eutectic compositions using molecular dynamic simulations. *RSC Adv.* **2016**, *6*, 59141–59149. [CrossRef]
10. He, Y.; Guo, X.; Long, Y.; Huang, G.; Ren, X.; Xu, C.; An, C. Inkjet Printing of GAP/NC/DNTF Based Microscale Booster with High Strength for PyroMEMS. *Micromachines* **2020**, *11*, 415. [CrossRef]
11. Song, L.; Zhao, F.; Xu, S.; Ju, X. Uncovering the action of ethanol controlled crystallization of 3, 4-bis (3-nitrofurazan-4-yl) furoxan crystal: A molecular dynamics study. *J. Mol. Graph. Model.* **2019**, *92*, 303–312. [CrossRef]
12. Sinditskii, V.P.; Burzhava, A.V.; Sheremetev, A.B.; Aleksandrova, N.S. Thermal and Combustion Properties of 3, 4-Bis (3-nitrofurazan-4-yl) furoxan (DNTF). *Propellants Explos. Pyrot.* **2012**, *37*, 575–580. [CrossRef]
13. Song, L.; Zhao, F.; Xu, S.; Ju, X.; Ye, C. Crystal Morphology of 3, 4-Bis (3-nitrofurazan-4-yl) furoxan in Methanol and Acetic Acid/Water Solutions by Spiral Growth Mechanism. *Propellants Explos. Pyrot.* **2020**, *45*, 1125–1136. [CrossRef]
14. Kazakov, A.I.; Dashko, D.V.; Nabatova, A.V.; Stepanov, A.; Lempert, D.B. Thermochemical and Energy Characteristics of DNTF and DNFF. *Combust. Explos. Shock* **2018**, *54*, 147–157. [CrossRef]
15. Gu, J.; Liu, L.; Chen, H.; Chen, W.; Guo, Z.; Chen, L. Study on the thermal decomposition kinetics of DNTF. E3S Web of Conferences. *EDP Sci.* **2021**, *245*, 01027.
16. Wu, Q.; Yang, C.; Pan, Y.; Xiang, F.; Liu, Z.; Zhu, W.; Xiao, H. First-principles study of the structural transformation, electronic structure, and optical properties of crystalline 2,6-diamino-3,5-dinitropyrazine-1-oxide under high pressure. *J. Mol. Model.* **2013**, *19*, 5159–5170. [CrossRef]
17. Wang, F.; Du, H.; Zhang, J.; Gong, X. First-Principle Study on High-Pressure Behavior of Crystalline Polyazido-1,3,5-triazine. *J. Phys. Chem. C* **2012**, *116*, 6745–6753. [CrossRef]
18. Wu, Q.; Zhu, W.; Xiao, H. Pressure effects on structural, electronic, absorption, and thermodynamic properties of crystalline 2,4,6-triamino-3,5-dinitropyridine-1-oxide: A DFT study. *J. Phys. Org. Chem.* **2013**, *26*, 589–595. [CrossRef]
19. Sun, F.; Zhang, G.; Ren, X.; Wang, M.; Xu, H.; Fu, Y.; Tang, Y.; Li, D. First-principles studies on phase stability, anisotropic elastic and electronic properties of Al-La binary system intermetallic compounds. *Mater. Today Commun.* **2020**, *24*, 101101. [CrossRef]
20. Wu, Q.; Zhu, W.; Xiao, H. First-principles study of the high-pressure behavior of solid 1, 7-diamino-1, 7-dinitrimino-2, 4, 6-trinitro-2, 4, 6-triazaheptane. *Comput. Chem.* **2014**, *1030*, 38–43. [CrossRef]
21. Wu, Q.; Zhu, W.; Xiao, H. Dispersion-corrected DFT study on the structure and absorption properties of crystalline 5-nitro-2,4-dihydro-1,2,4-triazole-3-one under compression. *Struct. Chem.* **2015**, *26*, 477–484. [CrossRef]
22. Sheremetev, A.B.; Ivanova, E.A.; Spiridonova, N.P.; Melnikova, S.F.; Tselinsky, I.V.; Suponitsky, K.Y.; Antipin, M.Y. Desilylative nitration of C, N-disilylated 3-amino-4-methylfurazan. *J. Heterocycl. Chem.* **2005**, *42*, 1237–1242. [CrossRef]
23. Mouhat, F.; Coudert, F.-X. Necessary and sufficient elastic stability conditions in various crystal systems. *Phys. Rev. B Condens. Matter Mater. Phys.* **2014**, *90*, 224104. [CrossRef]
24. Wang, W.; Liu, Q.; Liu, F.; Liu, Z. High-pressure structural, mechanical, and vibrational properties of NAPTO: The first fused-ring energetic material with a 2D layered structure. *Solid State Commun.* **2021**, *331*, 114293. [CrossRef]
25. Sun, F.; Zhang, G.; Liu, H.; Xu, H.; Fu, Y.; Li, D. Effect of transition-elements substitution on mechanical properties and electronic structures of B2-AlCu compounds. *Results Phys.* **2020**, *21*, 103765. [CrossRef]
26. Huang, B.; Duan, Y.; Hu, W.; Sun, Y.; Chen, S. Structural, anisotropic elastic and thermal properties of MB (M = Ti, Zr and Hf) monoborides. *Ceram. Int.* **2015**, *41*, 6831–6843. [CrossRef]
27. Liu, W.; Niu, Y.; Li, W. Theoretical prediction of the physical characteristic of Na_3MO_4 (M = Np and Pu): The first-principles calculations. *Ceram. Int.* **2020**, *46*, 25359–25365. [CrossRef]

28. Tian, J.; Zhao, Y.; Wen, Z.; Hou, H.; Han, P. Physical properties and Debye temperature of Al_7Cu_2Fe alloy under various pressures analyzed by first-principles. *Solid State Commun.* **2017**, *257*, 6–10. [CrossRef]
29. Zhu, W.H. First-principles band gap criterion for impact sensitivity of energetic crystals: A review. *Struct. Chem.* **2010**, *21*, 657–665. [CrossRef]